Journal Pre-proof

Ln^{3+} (Ln= Eu, Dy) -doped Sr_2CeO_4 fine phosphor particles: Wet chemical preparation, energy transfer and tunable luminescence

Na Gao, Yanfei Yang, Shikao Shi, Jiye Wang, Shuping Wang, Jibiao Li, Lianshe Fu

PII: S1002-0721(19)30658-1

DOI: https://doi.org/10.1016/j.jre.2019.09.014

Reference: JRE 620

To appear in: *Journal of Rare Earths*

Received Date: 2 August 2019

Revised Date: 19 September 2019

Accepted Date: 27 September 2019

Please cite this article as: Gao N, Yang Y, Shi S, Wang J, Wang S, Li J, Fu L, Ln^{3+} (Ln= Eu, Dy) -doped Sr_2CeO_4 fine phosphor particles: Wet chemical preparation, energy transfer and tunable luminescence, *Journal of Rare Earths*, https://doi.org/10.1016/j.jre.2019.09.014.

Ln^{3+} (Ln= Eu, Dy) –doped Sr_2CeO_4 fine phosphor particles: wet chemical preparation, energy transfer and tunable luminescence

Na Gao, Yanfei Yang, Shikao Shi, Jiye Wang, Shuping Wang, Jibiao Li, Lianshe Fu

The Ln^{3+} -doped Sr_2CeO_4 fine phosphor particles were successfully prepared with a consecutive hydrothermal and combustion reaction, and displayed tunable luminescence through an efficient energy transfer from the host to Ln^{3+}.

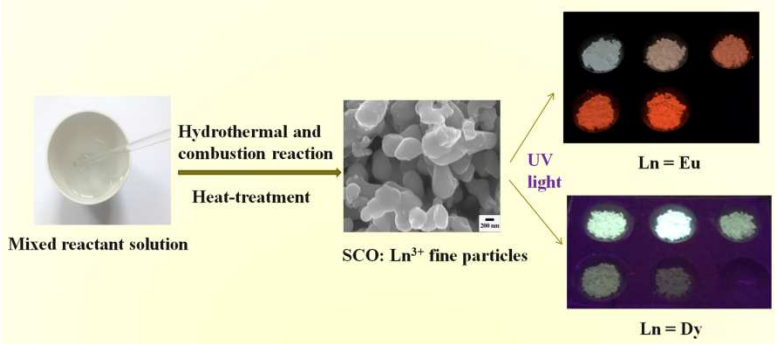

Ln^{3+} (Ln= Eu, Dy) -doped Sr_2CeO_4 fine phosphor particles: Wet chemical preparation, energy transfer and tunable luminescence

Na Gao [a], Yanfei Yang [a], Shikao Shi [a,*], Jiye Wang [a], Shuping Wang [a], Jibiao Li [a], Lianshe Fu [b]

[a]*Key Laboratory of Inorganic Nanomaterials of Hebei Province, College of Chemistry and Materials Science, Hebei Normal University, Shijiazhuang 050024, China*
[b]*Physics Department and CICECO - Aveiro Institute of Materials, University of Aveiro, 3810-193 Aveiro, Portugal*

Abstract The Sr_2CeO_4:Ln^{3+} (Ln= Eu, Dy) fine phosphor particles were prepared by a facile wet chemical approach, in which the consecutive hydrothermal-combustion reaction is performed. The doping of Ln^{3+} into Sr_2CeO_4 has little influence on the structure of host, and the as-prepared samples display well-crystallized spherical or elliptical shape with an average particle size at about 100 – 200 nm. For Eu^{3+} ions-doped Sr_2CeO_4, with the increase of Eu^{3+}-doping concentration, the blue light emission band with maximum at 468 nm originating from a $Ce^{4+}\rightarrow O^{2-}$ charge transfer of the host decreases obviously and the characteristic red light emission of Eu^{3+} ($^5D_0\rightarrow{}^7F_2$ transition at 618 nm) enhances gradually. Simultaneously, the fluorescent lifetime of the broadband emission of Sr_2CeO_4 decreases with the doping of Eu^{3+}, indicating an efficient energy transfer from the host to the doping Eu^{3+} ions. The energy transfer efficiency from the host to Eu^{3+} is investigated in detail, and the emitting color of Sr_2CeO_4:Eu^{3+} can be easily tuned from blue to red by varying the doping concentration of Eu^{3+} ions. Moreover, the luminescence of Dy^{3+}-doped Sr_2CeO_4 was also studied. Similar energy transfer phenomenon can be observed, and the incorporation of Dy^{3+} into Sr_2CeO_4 host leads to the characteristic emission of $^4F_{9/2}\rightarrow{}^6H_{15/2}$ (488 nm, blue light) and $^4F_{9/2}\rightarrow{}^6H_{13/2}$ (574 nm, yellow light) of Dy^{3+}. The Sr_2CeO_4:Ln^{3+} fine particles with tunable luminescence are quite beneficial for its potential applications in the optoelectronic fields.

Keywords: wet chemistry preparation; Sr_2CeO_4; Ln^{3+} ion; Phosphor; Luminescence; Energy transfer

Foundation item: Project supported by Natural Science Foundation of China (51972097)
[*]**Corresponding author**: E-mail address: shishikao@hebtu.edu.cn, Tel: +86-311-80787402

1. Introduction

It is well known that the inorganic luminescent materials are key components which are prerequisite to the functionality and success of plenty of lighting and display systems.[1] Two decades ago, a blue-light-emitting inorganic compound Sr_2CeO_4 (abbreviated as SCO), was first identified with combinatorial chemistry techniques by Golden group.[2,3] The compound contains an orthorhombic unit cell structure with one-dimensional chains of edge-sharing CeO_6 octahedra, and its luminescence originates from the charge transfer (CT) of $O^{2-} \rightarrow Ce^{4+}$, not from the 4f-5d transition of Ce^{3+}. Due to the unusual structure and luminescence properties of SCO, from then on, many interests are given to study the system.[4-7] Diverse approaches have been used to prepare the phosphor samples, such as the traditional high temperature solid state reaction,[8] sol-gel process,[9,10] solution combustion synthesis,[11,12] and microwave-assisted solvent thermal method.[13] However, some preparation approaches require high temperature and long reaction duration, leading to the irregular particles with serious aggregation. Even for the solution combustion reaction with a very short time, the as-prepared crystallites usually melt together because of the instantaneous crystallization process. The resulting inordinate shape does not meet the requirements in the practical optoelectronic fields. Therefore, it is necessary to further improve the preparation methods to achieve the fine particles with well-distributed morphology.

More recently, our group develops a novel wet chemical method which involves a consecutive hydrothermal and combustion reaction process to prepare SCO phosphor.[14] In the wet chemical preparation, the mixed urea and glycine (abbreviated as Gly) are both used as leavening agent and fuel in different process. By adjusting the molar ratio of urea: Gly and the sintering temperature, the crystallization and morphology of the particles are obviously improved, resulting in the as-prepared phosphors particles with well-distributed round shape and the average size at about 80-150 nm. Moreover, the phosphors with tunable luminescence are also highly desirable in the practical applications.[15] It has been reported that the energy transfer from O–Ce band to luminescent lanthanide ions (such as Sm^{3+}, Ho^{3+} and Yb^{3+}) can easily happen after the lanthanide ions are introduced to SCO, and the emitting color is changed.[11,16,17] Among the lanthanide ions, Eu^{3+} ion usually acts as an important activator in many phosphor systems due to its distinct red-emitting feature,[18] and the luminescence of Eu^{3+}-doped SCO is investigated by some groups, which may be applied for temperature and high pressure sensing as well as white light-emitting diodes.[19-22] In this paper, the lanthanide ions $Eu^{3+}$and Dy^{3+} ions are respectively incorporated to SCO host by the wet chemical method. Not only the fine uniform phosphor particles are achieved, but also the energy transfer from O–Ce band to luminescent Ln^{3+} ions is observed through the steady emission spectra and luminescent dynamics. The energy transfer efficiency from the host to Ln^{3+} ions and the Commission International de L'Eclairage (CIE) chromaticity coordinates of the samples are calculated. The emitting color of the Ln^{3+} –doped SCO can be varied from blue to red or other colors by adjusting the species and concentration of lanthanide ions, which is expected to use in the optoelectronic fields.

2. Experimental section

2.1. Preparation of samples

The raw materials in the work consist of $Sr(NO_3)_2$, $Ce(NO_3)_3{\cdot}6H_2O$ (both nitrates are from Yongda Chemical, Tianjin, 99.5%), Eu_2O_3 and Dy_2O_3 (the lanthanide oxides are all from Institute of Non-ferrous Metals, Beijing, 99.99%), urea (Analytical Reagent) and Gly (Biochemical Reagent). To achieve $Ln(NO_3)_3$ aqueous solutions (0.1 mol/L), their respective oxides are dissolved with dilute nitric acid. The other materials are used as received without further purification.

The wet chemical preparation of Eu^{3+} or Dy^{3+}-doped SCO fine particles contains a consecutive hydrothermal and combustion reaction process. Since the optimal molar ratio of urea to Gly has been confirmed to be 5:2 in the previously described,[14] the initial materials are first blended together in which the molar ratio of Sr:Eu (or Dy) : Ce : urea : Gly = $2-x$: x: 1 : 5 : 2 (x = 0.005–0.07), and dissolved with certain amount of distilled water. Then, the mixed aqueous solution is placed into a Teflon vessel to perform a hydrothermal reaction in an oven at 160 ^{o}C for 3 h. During the hydrothermal process, the urea and Gly are used as leavening agents to produce OH^- ions. The resulting OH^- ions tend to bind with metal ions to form precipitates, and therefore the solution and precipitates form a white emulsion. After the hydrothermal process, the as-prepared white emulsion as a precursor is transferred to a crucible to start a combustion reaction in a furnace. In the combustion reaction, the residual urea-Gly acts as fuel to ignite the precursor. Finally, the precursor powders are ground with an agate mortar, and moved to a corundum crucible to heat-treatment at 1000 ^{o}C for 3 h. In addition, the pure SCO is also prepared in the similar way for comparison purposes.

2.2. Characterization

The X-ray powder diffraction (XRD) patterns of the samples are measured with a Bruker D8 Advance X-ray diffractometer with Cu Kα (λ= 0.15406 nm) radiation at 40 kV and 40 mA over a 2θ scan range of 15 ^{o} –65^{o}. The morphology, particle size and energy dispersive X-ray spectroscopy (EDS) of the fine phosphors are analyzed using an S-4800 Hitachi field emission scanning electron microscope (SEM). The photoluminescence excitation and emission spectra of Eu^{3+} and Dy^{3+} -doped SCO are obtained through an F-4600 Hitachi spectrofluorometer equipped with a Xe lamp as the excitation source, and both the excitation and emission slits are 2.5 nm. The fluorescent decay curves and lifetimes are recorded using an FS5-TCSPC Edinburgh spectrofluorometer. All the measurements are carried out at ambient temperature.

3. Results and discussion

3.1 The structural and morphological characterization

The structure of SCO host has been indexed as an orthorhombic cell consisting of linear chains of edge-sharing CeO_6 octahedra. To investigate the effects of doping Ln^{3+} ion on the structure of the host, the XRD patterns of Eu^{3+}-doped (x = 0.005–0.07) SCO samples were measured and are shown

in Fig. 1. As can be seen from Fig. 1, the main diffraction peaks at 16.9°, 29.4°, 29.8°, 30.2°, 42.6° and 53.3° belong to the (110), (220), (130), (111), (221) and (151) planes of SCO, respectively. Since the data are almost in agreement with the JCPDS 50-0115, the formation of phase SCO is identified and the introduction of certain amount of Eu^{3+} into the lattice has little influence on the formation of SCO. Additionally, the XRD patterns of Dy^{3+}-doped (x = 0.005–0.07) SCO samples are also measured and given in supplementary information 1. The XRD data have the similar results with Fig. 1, indicating that the incorporation of certain amount of Ln^{3+} ion into the lattice cannot make obvious influence on the structure of SCO.

To observe the morphology, size and composition of Ln^{3+}-doped SCO samples, the SEM and EDS of $0.07Ln^{3+}$ (Ln= Eu,Dy)-doped SCO are shown in Fig. 2. In SEM of Fig.2(a,b), most phosphor particles have well-crystallized round or elliptical shape and the particle diameter are around 100 – 200 nm, despite a few particles are bound together. Furthermore, the EDS results of Fig. 2(c, d) reveal the existence of Sr, Ce and O elements in the host as well as the doping Eu and Dy elements. In comparison with the SEM of the pure SCO samples prepared with this method,[14] it can be concluded that the small amount doping of Ln^{3+} into SCO host has little effect on its morphology and size. The Ln^{3+}-doped Sr_2CeO_4 phosphor particles with well-distributed shape and uniform size are welcome in the practical uses.

3.2. Luminescence properties

The luminescent properties of Eu^{3+}-doped SCO phosphor particles are investigated in detail. Figs. 3,4 exhibit the excitation and emission spectra of SCO:$x$$Eu^{3+}$ (x= 0.005–0.07), respectively. Without considering the change of relative intensity, the shape of the excitation and emission spectra is independent with the Eu^{3+} doping concentration. Monitored with the characteristic emission ($^5D_0 \rightarrow {}^7F_2$ transition at 618 nm) of Eu^{3+}, an evident broadband from 200 to 400 nm with peak at about 277 nm as well as some weak peaks at 395 and 466 nm can be observed in the excitation spectra (Fig. 3). The broadband with peak at about 277 nm is attributed to the $O^{2-} \rightarrow Ce^{4+}$ CT transition in the host,[23] and the tiny peaks around 395 and 466 nm belong to the intrinsic transition of $^7F_0 \rightarrow {}^5L_6$ and $^7F_0 \rightarrow {}^5D_2$ of Eu^{3+}, respectively.[24] Since the broadband peak around 277 nm is much stronger than the tiny intrinsic transitions of Eu^{3+}, the UV 277 nm is a suitable choice as the optimal excitation wavelength in the following studies.

In the emission spectra of Fig. 4 (λ_{ex}= 277 nm), the SCO: Eu^{3+} phosphor particles can emit a broadband from 400 to 600 nm and quite a few narrow bands. The broadband with the maximum at 468 nm originates from the CT transition of $Ce^{4+} \rightarrow O^{2-}$, which produces blue light emission and is almost the same with that of the pure SCO. While the narrow bands are assigned to three series of transitions of Eu^{3+}, $^5D_2 \rightarrow {}^7F_J$ (J= 0, 2, 3), $^5D_1 \rightarrow {}^7F_J$ (J= 1, 2) and $^5D_0 \rightarrow {}^7F_J$ (J= 1, 2, 3, 4), respectively. The former two series of transition peaks from higher excited state ($^5D_2$ and $^5D_1$) to ^7F_J at 467, 491, 512, 537 and 556 nm (between 460 to 560 nm) are all attached to the top of the CT broadband emission, and the latter series of transition peaks from lower excited state $^5D_0$ to ^7F_J (J= 1, 2, 3, 4) locate at 585, 618, 656 and 706 nm, respectively. Among the $^5D_0 \rightarrow {}^7F_J$ transitions, the dominant one is $^5D_0 \rightarrow {}^7F_2$ transition emission at 618 nm (red light region).

To more clearly elucidate the variation trends of the main emission peaks in Fig. 4, the dependence of relative emission intensity of CT broadband and $^5D_0 \rightarrow {}^7F_2$ transition (at 618 nm) with Eu^{3+} doping concentration (x) is plotted in Fig. 5. It can be observed from Fig. 5 that the CT broadband emission intensity is higher than the $^5D_0 \rightarrow {}^7F_2$ transition emission when Eu^{3+} is doped at very low concentration (x= 0.005). However, with the increase of Eu^{3+} doping concentration, the CT broadband emission intensity decreases gradually, and the $^5D_0 \rightarrow {}^7F_2$ transition emission at 618 nm is enhanced and exceeds the broadband emission immediately. As the Eu^{3+} doping concentration reaches x= 0.07, the CT broadband gets very weak and the $^5D_0 \rightarrow {}^7F_2$ transition emission peak at 618 nm turns into the predominant role among all the emission transitions. It is inferred from the result that the increase of Eu^{3+} doping concentration leads to the decrease of CT broadband emission as well as the enhancement of the $^5D_0 \rightarrow {}^7F_2$ transition emission of Eu^{3+}, and therefore an energy transfer phenomenon from the SCO host to Eu^{3+} is inevitably to happen.

The emission intensity ratio (I_{618}/I_{585}) for $^5D_0 \rightarrow {}^7F_2$ (618 nm) to $^5D_0 \rightarrow {}^7F_1$ (585 nm) of Eu^{3+} is often used to probe the symmetry of Eu^{3+} in the host lattice due to their distinct properties. It is known that the $^5D_0 \rightarrow {}^7F_2$ transition is a forced-electric dipole transition, and the $^5D_0 \rightarrow {}^7F_1$ transition is allowed according to the magnetic dipole selection rule.[25] The forced-electric dipole transition intensity is quite sensitive to the local environment around Eu^{3+} ions. On the contrary, the latter magnetic dipole transition intensity is relatively independent of the site symmetry and surroundings of Eu^{3+} ions. Thus, the higher the I_{618}/I_{585} value, the more Eu^{3+} would occupy sites without an inversion centre.[26] The I_{618}/I_{585} values for Eu^{3+}–doped SCO samples are listed in Table 1. It is evidently that the I_{618}/I_{585} value is always more than 1, and the I_{618}/I_{585} value is gradually increased with the increase of Eu^{3+} doping concentration (x). In other words, more and more Eu^{3+} would occupy sites without inversion symmetry with the increase of the Eu^{3+} doping concentration (x).

To investigate the effects of the Eu^{3+} doping concentration (x) on the energy transfer efficiency (η_T) from SCO to Eu^{3+}, the fluorescent decay curves of the pure SCO and SCO:$x$$Eu^{3+}$ (x= 0.005–0.07) are measured (λ_{ex}= 277 nm, λ_{em}= 450 nm). The reason for selecting the monitored wavelength as 450 nm (not the maximum 468 nm of the broadband emission) is to eliminate the interference of Eu^{3+} emission. Fig. 6 gives the fluorescent decay curves of SCO and SCO: 0.005Eu^{3+}. Both the decay curves are well fitted with a single-exponential function, implying that the Ce^{4+} ions locate only one type of the lattice site. However, the lifetime (τ) value (17.4 μs) of SCO: 0.005Eu^{3+} is obviously smaller than that of the pure SCO (35.3 μs) despite a very low Eu^{3+} doping concentration. With the increase of Eu^{3+} doping concentration (x), the τ value is further reduced (see Table 1). As Eu^{3+} doping concentration x= 0.07, the τ value is lowered to 3.6 μs. The η_T can be calculated with the following equation:[27,28]

$$\eta_T = 1 - \left(\frac{\tau}{\tau_0} \right) \quad (1)$$

In the equation (1), the τ and τ_0 value is the fluorescent lifetime of SCO host in the presence and absence of Eu^{3+}. The calculated η_T value of the samples is also listed in Table 1. As x is 0.005, the η_T value is 50.7%. With the x increases from 0.01, 0.03, 0.05 and 0.07, the η_T value is gradually increased to 67.7%, 79.6%, 87.5% and 89.8%, respectively. This means that the energy transfer

efficiency is effectively improved with the increase of Eu^{3+} doping concentration, and the emitting color of SCO:Eu^{3+} can be tuned by changing the Eu^{3+} doping concentration.

To intuitively observe the emitting color variation of Eu^{3+}-doped SCO phosphor particles due to the energy transfer phenomenon from the host to Eu^{3+}, the luminescence images of the above samples irradiated with 254 nm UV light are shown in Fig. 7. Simultaneously, the CIE chromaticity coordinates of the samples are calculated and shown in Fig. 8 (a) (The CIE coordinate value is listed in Table 1). As can be seen from Fig. 7 and 8 (a), the doping of Eu^{3+} in different concentrations adjusts the bluish-white light of the host itself. With the increase of Eu^{3+} doping concentration, the emitting color is varied from bluish-white to pale-white, then to red light. The reason for producing white light is due to the combination of three emission transitions of red (618 nm), green (537 nm) and blue (467 nm) light.

Dy^{3+} is also an important Ln^{3+} ion in the rare earth luminescence of phosphors,[15] and the photoluminescence and energy transfer of Dy^{3+}-doped SCO phosphor particles are investigated. The excitation spectra shape (λ_{em}= 574 nm) of Dy^{3+}-doped SCO samples (see supplementary information 2) are almost the same with that of Fig. 3, which shows an evident broadband transition from 200 to 400 nm with peak at about 277 nm, no matter the Dy^{3+} doping concentration is low or high. Due to the doping of Dy^{3+}, the weak peaks at 395 and 466 nm belonging to the Eu^{3+} transitions in Fig. 3 are not observed. No doubt, this excitation broadband originates from the $O^{2-} \rightarrow Ce^{4+}$ CT transition in the host.

Excited with UV 277 nm, the emission spectra of Dy^{3+}-doped SCO phosphor particles (Fig. 9) exhibit not only a broadband between 400 to 600 nm, but also three narrow band peaks. The broadband emission belongs to the CT transition of Ce^{4+} in the host itself, and the three narrow band peaks at about 488, 574 and 667 nm correspond to the $^4F_{9/2} \rightarrow {}^6H_{15/2}$, $^4F_{9/2} \rightarrow {}^6H_{13/2}$ and $^4F_{9/2} \rightarrow {}^6H_{13/2}$ characteristic transition emissions of Dy^{3+} ions,[29,30] respectively. Among the three narrow band peaks, the Dy^{3+} emission at 574 nm (yellow light) is a prominent peak, and the one at 667 nm looks very weak. Moreover, the Dy^{3+} emission at 488 nm (blue light) is seriously overlapped with the host broadband emission. After Dy^{3+} is incorporated into SCO, the broadband emission of the host itself is greatly decreased and with the increase of Dy^{3+} doping concentration (as x>0.01), the broadband emission is gradually decreased, which indicates the energy transfer happens from the host to Dy^{3+}. Additionally, the emission intensity dependence of Dy^{3+} at 488 and 574 nm with Dy^{3+} doping concentration has the similar change trend with the broadband of SCO host (Fig. 10), which is quite different from the $^5D_0 \rightarrow {}^7F_2$ (618 nm) transition emission of Eu^{3+} in Fig. 5. The reason for the difference may concern two aspects. (1) Emission peak locations. Both the characteristic emission peaks of Dy^{3+} at 488 and 574 nm particularly the one at 488 nm are overlapped with the broadband emission of SCO host, but the characteristic emission of Eu^{3+} at 618 nm is well-separated with the broadband emission. (2) Quenching concentrations. In the previous literatures,[8,31] the luminescence quenching concentration of Dy^{3+} (about 0.0075) is far less than that of Eu^{3+} (x>0.10) in SCO. In this work, the doping concentration range for Ln^{3+} is from 0 to 0.07, and our result does not contradict with the previous reports. As a consequence, the characteristic emission intensity of Eu^{3+} at 618 nm is always enhanced with the increase of Eu^{3+} doping concentration, while the characteristic emission

of Dy^{3+} at 488 and 574 nm is reduced as x>0.01.

The fluorescent lifetimes (τ) of SCO host samples after the doping of Dy^{3+} are measured and the energy transfer efficiency (η_T) from SCO host to Dy^{3+} are calculated according to Eq. (1), and listed in Table 2. As Dy^{3+} is doped to SCO, the τ value is dramatically reduced (< 5 μs), and therefore results in very high energy transfer efficiency from SCO host to Dy^{3+}. For example, the η_T value can reach 92.3% as the doping concentration of x= 0.03. Due to the prominent emission of Dy^{3+} at yellow light region, the emitting color of the SCO: Dy samples under the irradiation with UV light can be tuned from bluish-white to yellowish-green, as can be seen from Fig. 11. As the doping concentration of Dy^{3+} is high as 0.07, the emitting intensity gets very weak due to the heavy concentration quenching effect. Moreover, for the convenience of comparison, the CIE chromaticity coordinates of the Dy^{3+}-doped SCO samples are also calculated and shown in Fig. 8 (b) (The CIE coordinate value is listed in Table 2).

The energy transfer and electronic transitions in SCO: Ln^{3+} (Eu^{3+}, Dy^{3+}) are illustrated with the schematic energy-level diagram (Fig. 12). Upon the incidence with 277 nm UV light, the photon energy is absorbed by the SCO host, and the host is excited from the ground state (GS) to $O^{2-}\rightarrow Ce^{4+}$ ligand-to-metal charge transfer (LMCT) low spin state (LS). Then the excitation is promptly relaxed to LMCT high spin state (HS) with slightly lower energy. On the other hand, the broadband emission with the peak at 468 nm is associated with the $Ce^{4+}\rightarrow O^{2-}$ metal-to-ligand charge transfer (MLCT), which means the radiative relaxation of MLCT to the GS leading to the blue light emission. It is evidently that the energy of MLCT state is very close to the excited state of $^5D_2$ of Eu^{3+} and $^4I_{15/2}$ of Dy^{3+} ions.[32] Thus, the incorporation of Eu^{3+} or Dy^{3+} ions into the SCO host facilitates the energy transfer from MLCT to the excited state of $^5D_2$ of Eu^{3+} and $^4I_{15/2}$ of Dy^{3+} ions. As a result, the characteristic transition emissions of Eu^{3+} and Dy^{3+} take place, which correspond to those in Figs. 4 and 9, respectively. With the increase of Ln^{3+} doping concentration, more and more energy from MLCT state are transferred to Ln^{3+}, and the energy transfer efficiency is gradually improved. Additionally, in the case of SCO: Eu3+ phosphor particles, once the electrons are pumped into the LS, the energy absorbed by the LMCT transition will transfer to the $Eu^{3+}\rightarrow O^{2-}$ charge transfer state by the dipole–dipole interaction type according to the Inokuti–Hirayama theory.[33] The energy then arrives at ^5D_J (J=0, 1, 2) level of Eu^{3+} by non-radiative transition. As a consequence, the transferred energy leads to the emission from all $^5D_0$, $^5D_1$ and $^5D_2$ levels of Eu^{3+} ions.

To more clearly clarify the energy transfer phenomenon from SCO to Ln^{3+}, the emission spectra (λ_{ex}= 277 nm) of pure SCO host, SCO:0.07Eu^{3+} and SCO: 0.005Dy^{3+} (the corresponding images irradiated with a 254 nm UV light are also given) are compared in Fig. 13. The pure SCO host produces blue light with an intense broadband emission. For Ln^{3+}-doped SCO samples, the blue emission of SCO itself is markedly reduced due to the efficient energy transfer process from SCO host to Ln^{3+}. As Eu^{3+} doping concentration is as high as 0.07, its energy is basically transferred to the activator Eu^{3+}, resulting in the red-light-emitting of $^5D_0\rightarrow{}^7F_2$ transition with dramatic enhancement. Even for SCO:0.005Dy^{3+} sample, in which the Dy^{3+} doping concentration is very low, the energy transfer from SCO host to Dy^{3+} is quite enough to diminish the broadband emission of

the host and leads to the prominent $^4F_{9/2}\rightarrow{}^6H_{13/2}$ emission of Dy^{3+} at yellow light region. Accompanied with the $^4F_{9/2}\rightarrow{}^6H_{15/2}$ emission of Dy^{3+} at blue light region, the emitting color of SCO:0.005Dy^{3+} sample shows yellowish-green.

4. Conclusion

We successfully prepared Ln^{3+} (Ln= Eu, Dy)-doped SCO fine phosphor particles by consecutive hydrothermal-combustion reaction as well as a heat-treatment process at 1000 ^oC. The phosphor samples show spherical or elliptical shape with good crystallization, and the particle diameters are around 100 – 200 nm. It is found that the certain amount ($0<x<0.07$) of Ln^{3+} into SCO has little influence on the structure of host. However, the optical performances of SCO:Ln^{3+} are quite different from SCO host. The luminescence of SCO host itself has a blue broadband emission originating from the MLCT of $Ce^{4+}\rightarrow O^{2-}$. After Ln^{3+} ions are incorporated into SCO host, an efficient energy transfer process from the SCO host to Ln^{3+} can easily happen due to the energy of MLCT very close to the excited state of $^5D_2$ of Eu^{3+} and $^4I_{15/2}$ of Dy^{3+} ions, which is confirmed through the steady emission spectra and luminescent decay dynamics. Consequently, the emitting color of SCO:Eu^{3+} can be tuned from blue to red ($^5D_0\rightarrow{}^7F_2$ transition at 618 nm) by varying the doping concentration of Eu^{3+} ions, and the emitting color of SCO:Dy^{3+} can be changed to yellowish-green due to the co-existence of $^4F_{9/2}\rightarrow{}^6H_{13/2}$ (574 nm, yellow light) and $^4F_{9/2}\rightarrow{}^6H_{15/2}$ (488 nm, blue light) emission transitions. The Ln^{3+}-doped SCO fine phosphor particles with tunable luminescence exhibit promising inorganic luminescent materials in the optoelectronic fields.

Acknowledgments

This work was financially supported the Science Foundation of Hebei Normal University, China (L2019K11). This work was also financially supported by the project WINLEDS—POCI-01-0145-FEDER-030351 and developed within the scope of the project CICECO-Aveiro Institute of Materials, FCT Ref. UID/CTM/50011/2019, financed by national funds through the FCT/MCTES.

References

1 Feldmann C, Jüstel T, Ronda C R, Schmidt P J. Inorganic luminescent materials: 100 years of research and application, Adv Funct Mater. 2003, 13: 511.

2 Danielson E, Devenney M, Giaquinta D M, Golden J H, Haushalter R C, McFarland EW, et al. A rare-earth phosphor containing one-dimensional chains identified through combinatorial methods, Science. 1998, 279: 837.

3 Danielson E, Devenney M, Giaquinta D M, Golden J H, Haushalter R C, McFarland EW, et al. X-ray powder structure of Sr_2CeO_4: a new luminescent material discovered by combinatorial

chemistry, J Mol Struct. 1998, 470: 229.
4 Li L, Zhou S H, Zhang SY. Investigation on charge transfer bands of Ce^{4+} in Sr_2CeO_4 blue phosphor, Chem Phys Lett. 2008, 453: 283.
5 Hirai T, Kawamura Y. Preparation of Sr_2CeO_4 blue phosphor particles and rare earth (Eu, Ho, Tm, or Er)-doped Sr_2CeO_4 phosphor particles, using an emulsion Liquid Membrane System. J Phys Chem B. 108 (2004) 12763–12769.
6 Stefanski M, Marciniak L, Hreniak D, Strek W. Influence of grain size on optical properties of Sr_2CeO_4 nanocrystals, J Chem Phys. 2015, 142: 184701.
7 Wen D W, Kato H, Kobayashi M, Yamamoto S, Mitsuishi M, Fujii K, et al. Ce^{4+}-based compounds capable of photoluminescence by charge transfer excitation under near-ultraviolet-visible light, Inorg Chem. 2018, 57: 14524.
8 Mu Z F, Hu Y H, Chen L, Wang X J. Enhanced red emission in Sr_2CeO_4:Eu^{3+} by Charge Compensation, J Electrochem Soc. 2011, 158: J287.
9 Strek W, Tomala R, Marciniak L, Lukaszewicz M, Cichy B, Stefanski M, et al. Broadband anti-Stokes white emission of Sr_2CeO_4 nanocrystals induced by laser irradiation, Phys Chem Chem Phys. 2016, 18: 27921.
10 Stefanski M, Lukaszewicz M, Hreniak D, Strek W, Laser induced white emission generated by infrared excitation from Eu^{3+}:Sr_2CeO_4 nanocrystals, J Chem Phys. 2017, 146: 104705.
11 Monika D L, Nagabhushana H, Sharma S C, Nagabhushana B M, Krishna R H. Synthesis of multicolor emitting $Sr_{2-x}Sm_xCeO_4$ nanophosphor with compositionally tunable photo and thermoluminescence, Chem Engin J. 2014, 253: 155.
12 Vlasic A, Sevic D, Rabasovic M S, Krizan J, Savic-Sevic S, Rabasovic M D, et al. Effects of temperature and pressure on luminescent properties of Sr_2CeO_4:Eu^{3+} nanophosphor, J Lumin. 2018, 199: 285.
13 Lu C H, Wu T Y, Hsu C H. Synthesis and photoluminescent characteristics of Sr_2CeO_4 phosphors prepared via a microwave-assisted solvothermal process, J Lumin. 2010, 130: 737.
14 Yang Y F, Zuo X Y, Shi S K, Li J B, Wang J Y, Geng L N, et al. Hydrothermal combustion synthesis and characterization of Sr_2CeO_4 phosphor powders, Mater Res Bull. 2019, 112: 159.
15 Li K, Shang M M, Lian H Z, Lin J. Recent development in phosphors with different emitting colors via energy transfer, J Mater Chem C. 2016, 4: 5507.
16 Monika D L, Nagabhushana H, Nagabhushana B M, Sharma S C, Anantharaju K S, Daruka Prasad B, et al. One pot auto-ignition based synthesis of novel Sr_2CeO_4: Ho^{3+} nanophosphor for photoluminescent applications, J Alloys Compd. 2015, 648: 1051.
17 Zhou R, Wei X T, Chen Y H, Duan C K, Yin M. Ultraviolet to near-infrared downconversion inYb^{3+}-doped Sr_2CeO_4. Phys Status Solidi B. 2012, 249: 818.
18 Tu D T, Zheng W, Huang P, Chen X Y. Europium-activated luminescent nanoprobes: from fundamentals to bioapplications, Coordin Chem Rev. 2019, 378: 104.
19 Shi L, Zhang H J, Li C Y, Su Q. Eu^{3+} doped Sr_2CeO_4 phosphors for thermometry: single-color or two-color fluorescence based temperature characterization, RSC Adv. 2011, 1: 298.

20 Gupta S K, Sahu M, Krishnan K, Saxena M K, Natarajana V, Godbole S V. Bluish white emitting Sr_2CeO_4 and red emitting Sr_2CeO_4:Eu^{3+} nanoparticles: optimization of synthesis parameters, characterization, energy transfer and photoluminescence, J Mater Chem C. 2013, 1: 7054.

21 Li H F, Zhao R, Jia Y L, Sun W Z, Fu J P, Jiang L H, et al. $Sr_{1.7}Zn_{0.3}CeO_4$: Eu^{3+} novel red-emitting phosphors: synthesis and photoluminescence properties, ACS Appl. Mater. Interfaces 2014, 6: 3163.

22 Stefanski M, Marciniak L, Hreniak D, Strek W. Size and temperature dependence of optical properties of Eu^{3+}:Sr_2CeO_4 nanocrystals for their application in luminescence thermometry, Mater Res Bull. 2016, 76: 133.

23 van Pieterson L, Soverna S, Meijerink A. On the nature of the luminescence of Sr_2CeO_4, J Electrochem Soc. 2000, 147: 4688.

24 Shi S K, Li K Y, Wang S P, Zong R L, Zhang G L. Structural characterization and enhanced luminescence of Eu-doped $2CeO_2$–$0.5La_2O_3$ composite phosphor powders by a facile solution combustion synthesis, J Mater Chem C. 2017, 5: 4302.

25Tanner P A. Some misconceptions concerning the electronic spectra of tri-positive europium and cerium, Chem Soc Rev. 2013, 42: 5090.

26 Shi S K, Hossu M, Hall R, Chen W. Solution combustion synthesis, photoluminescence and X-ray luminescence of Eu-doped nanoceria CeO_2: Eu, J Mater Chem. 2012, 22: 23461.

27 Shang M M, Li G G, Kang X J, Yang D M, Geng D L, Lin J. Tunable luminescence and energy transfer properties of Sr_3AlO_4F: RE^{3+} (RE = Tm/Tb, Eu, Ce) Phosphors, ACS Appl Mater Interfaces. 2011, 3: 2738.

28 Shi S K, Zhang X J, Wang S P, Geng L N, Zhang J J, Chen W. Precipitation synthesis and color-tailorable luminescence of a-$Zr(HPO_4)_2$:RE^{3+} (RE = Eu, Tb) nanosheet phosphors, J Am Ceram Soc. 2015, 98: 3836.

29 Ukare R S, Dubey V, Zade G D, Dhoble S J. PL properties of Sr_2CeO_4 with Eu^{3+} and Dy^{3+} for solid state lighting prepared by precipitation method, J Fluoresc. 2016, 26: 791.

30 Rajendra H J, Pandurangappa C, Monika D L. Luminescence properties of dysprosium doped YVO_4 phosphor, J Rare Earths 2018, 36: 1245.

31 Monika D L, Nagabhushana H, Krishna R H, Nagabhushana B M, Sharma S C, Thomas T. Synthesis and photoluminescence properties of a novel Sr_2CeO_4 :Dy^{3+} nanophosphor with enhanced brightness by Li^+ co-doping, RSC Adv. 2014, 4: 38655.

32 Blasse G, Grambmaier B C. Luminescent Materials, first ed., Springer-Verlag, Berlin, 1994. 26.

33 Li H F, Jia Y L, Sun W Z, Zhao R, Fu J P, Jiang LH, Zhang S, Pang R, Li C Y. Novel energy transfer mechanism in single-phased color-tunable Sr_2CeO_4:Eu^{3+} phosphors for WLEDs, Opt Mater. 2014, 36: 1883.

Figure captions

Fig. 1. XRD patterns of the SCO:xEu^{3+}phosphor particles (x=0.005 to 0.07).

Fig. 2. SEM images (a, b) and EDS spectra (c, d) of Ln^{3+} (Ln= Eu, Dy) –doped SCO phosphor particles.

Fig. 3. Excitation spectra (λ_{em}= 618 nm) of SCO: xEu^{3+}phosphor particles (x=0.005 to 0.07).

Fig. 4. Emission spectra (λ_{em}= 277 nm) of SCO: xEu^{3+}phosphor particles (x=0.005 to 0.07).

Fig. 5. Dependence of the relative emission intensity of CT broadband (at 450 nm) and $^5D_0 \rightarrow {}^7F_2$ transition (at 618 nm) with Eu^{3+} doping concentration (x) for SCO:xEu^{3+} samples.

Fig. 6. The fluorescent decay curves of SCO (1) and SCO: 0.005Eu^{3+} (2) phosphor samples (λ_{ex}= 277 nm; λ_{em}= 450 nm).

Fig. 7. The luminescence images of SCO:xEu^{3+} phosphor particles irradiated with a 254 nm UV lamp. (a) x= 0.005; (b) x= 0.01; (c) x= 0.03; (d) x= 0.05; (e) x=0.07.

Fig. 8. CIE coordinate diagram of Ln^{3+}-doped SCO phosphor samples. (a) Ln= Eu; (b) Ln= Dy.

Fig. 9. Emission spectra (λ_{em}= 277 nm) of SCO:xDy^{3+}phosphor particles (x=0.005 to 0.07).

Fig. 10. Dependence of the relative emission intensity at 450, 488 and 574 nm with Dy^{3+} doping concentration (x) for SCO:xDy^{3+} samples.

Fig. 11. The luminescence images of SCO:xDy^{3+} phosphor particles irradiated with a 254 nm UV lamp. (a) x= 0.005; (b) x= 0.01; (c) x= 0.03; (d) x= 0.05; (e) x= 0.07.

Fig. 12. The schematic diagram of energy transfer and electronic transitions in SCO:Ln^{3+} (Ln= Eu, Dy) phosphor particles. LS, HS and GS mean the low spin state, high spin state and ground state, respectively.

Fig. 13 Emission spectra (λ_{ex}= 277 nm) comparison and the corresponding images irradiated with a 254 nm UV light of pure SCO host, SCO:0.07Eu^{3+} and SCO:0.005Dy^{3+}.

Table 1. Some optical parameters of Eu^{3+}-doped SCO phosphor samples

Eu^{3+} doping concentration (x)	I_{618}/ I_{585}	τ (μs)	η_T (%)	CIE coordinate	
				X	*Y*
0.005	1.31	17.4	50.7	0.228	0.272
0.01	1.85	11.4	67.7	0.281	0.299
0.03	2.81	7.2	79.6	0.385	0.327
0.05	3.17	4.4	87.5	0.498	0.338
0.07	3.44	3.6	89.8	0.553	0.338

Table 2. Some optical parameters of Dy^{3+}-doped SCO phosphor samples

Dy^{3+} doping concentration (x)	τ (μs)	η_T (%)	CIE coordinate	
			X	*Y*
0.005	3.1	91.2	0.269	0.307
0.01	4.8	86.4	0.242	0.288
0.03	2.7	92.3	0.276	0.309
0.05	1.8	94.9	0.282	0.307
0.07	1.3	96.3	0.245	0.263

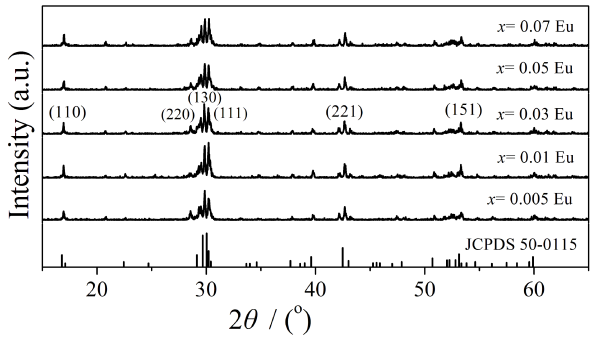

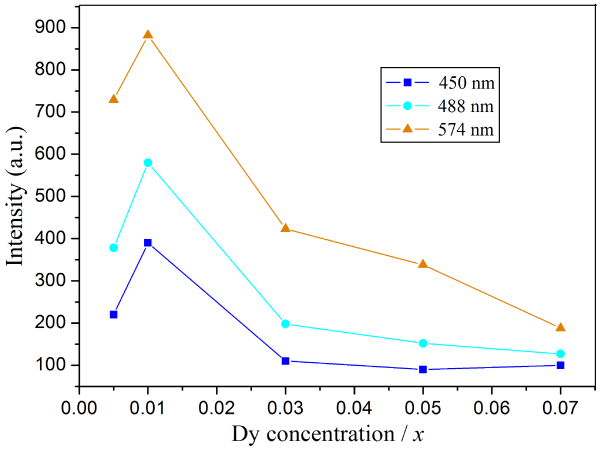

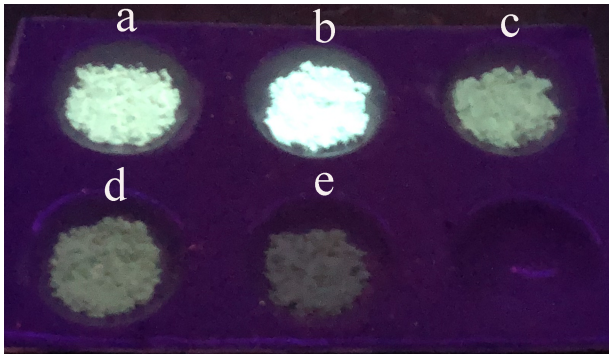

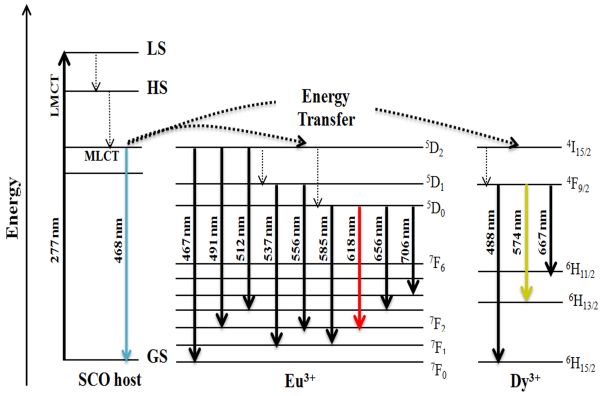

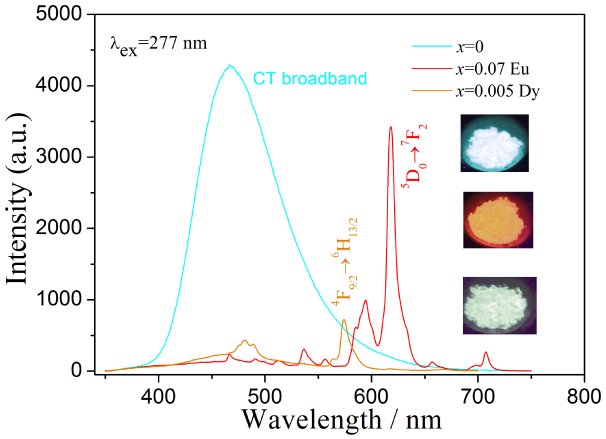

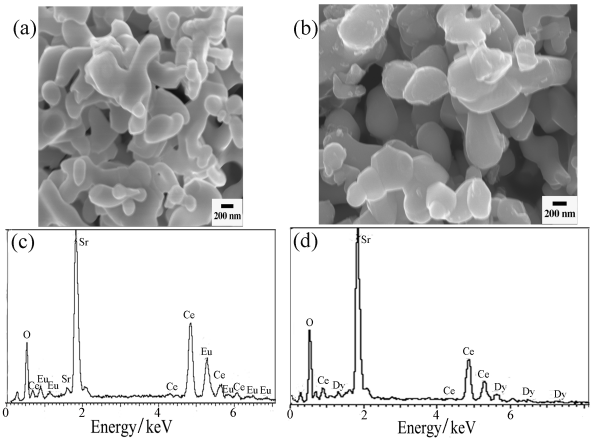

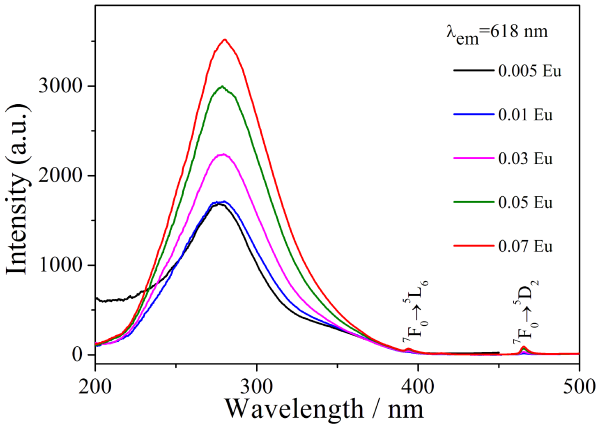

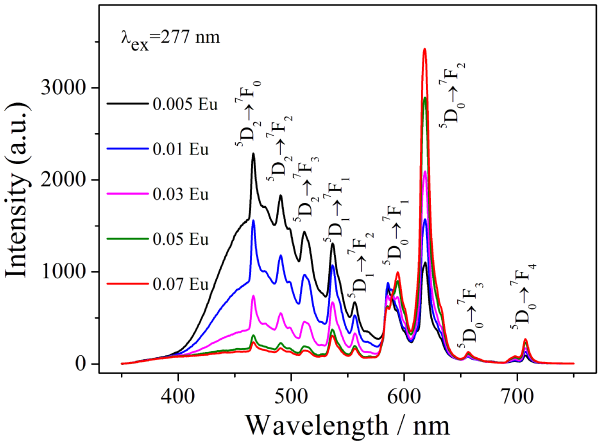

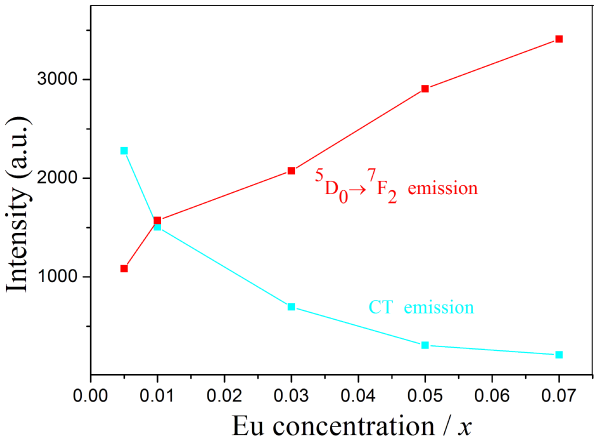

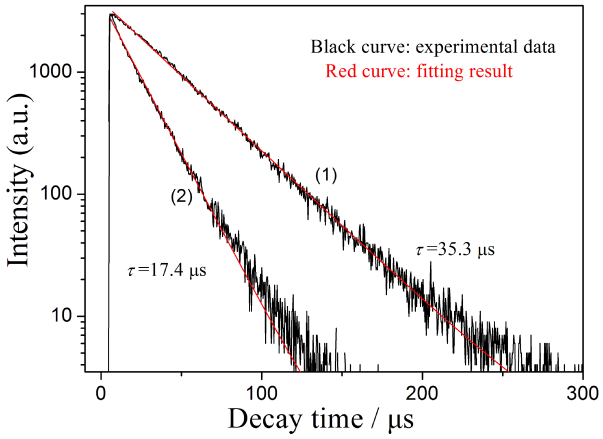

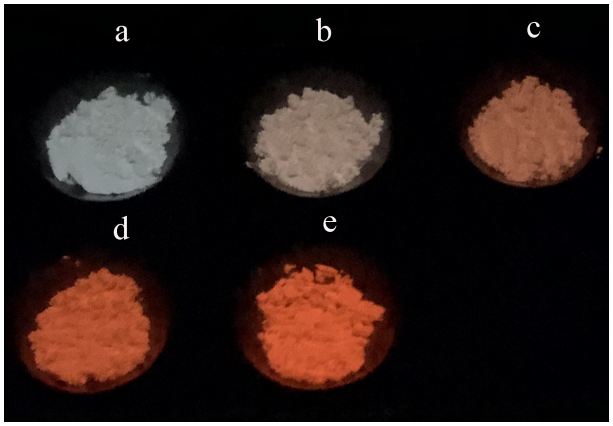

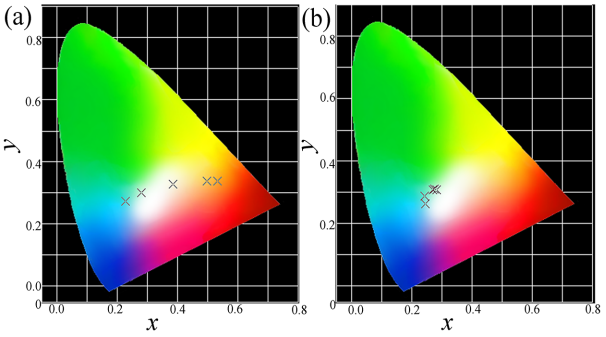

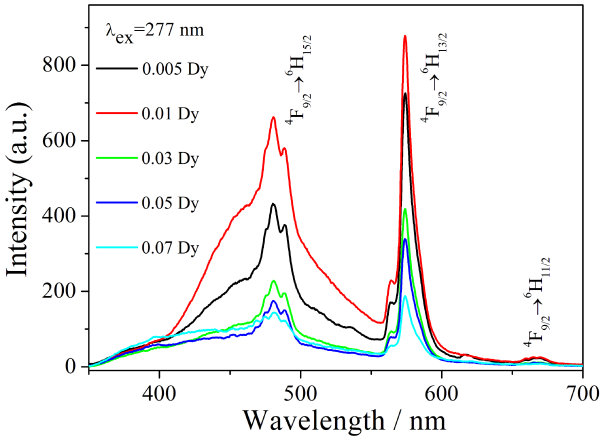

Conflict of Interest

As the corresponding author of the manuscript, I declare that all the authors have no conflicts of interest to this work.

Shikao Shi

from Hebei Normal University, China